

Performance analysis for direct 2-propanol fuel-cell based on Pt containing anode electrocatalysts

Niyazi Alper TAPAN^{*}, Ezgi ÖZTÜRK

*Department of Chemical Engineering, Faculty of Engineering & Architecture,
Gazi University, 06570 Maltepe, Ankara-TURKEY
e-mail: atapan@gazi.edu.tr*

Received 17.09.2008

Direct 2-propanol cell performance based on Pt containing anode electrocatalyst was evaluated. Cell performance, open circuit voltage, maximum current density, and maximum power density were measured at various alcohol concentrations and cell temperatures. 2-propanol fuel cell shows the highest performance at 1 M concentration and 80 °C operating temperature. The highest practical efficiency (at the maximum power density) was found at 2 M 2-propanol concentration and 60 °C operating temperature. Parameter estimation was performed by non-linear least squares method using the Levenberg Marquardt algorithm. According to the parametric analysis, cross-over current was minimum for 0.5 M 2-propanol concentration at 40 °C operating temperature.

Key Words: Propanol, Fuel cell, Performance, Electrocatalyst.

Introduction

Nowadays, world energy demand is continuously increasing due to expanding industrialization. In order to meet this demand effectively, alternative energy sources are needed instead of fossil fuels. PEM fuel cells are one of the tools that can overcome this energy issue.

PEM (polymer electrolyte membrane) fuel cells are preferred as they are not limited by Carnot efficiency and can operate at low temperatures. Especially direct alcohol fuel cells do not have any fuel storage, fuel processing problems, and they have high fuel energy densities. On the other hand, direct alcohol fuel cells have some drawbacks like alcohol cross-over and poisoning of anode electrode by decomposition of products during fuel cell operation. Therefore, to minimize the problems mentioned above, higher alcohols like 2-propanol should

*Corresponding author

be investigated. The analysis of thermodynamic-energetic data and toxicological-ecological hazard of liquid fuels show that 2-propanol is one of the most adequate liquid fuels for the polymer electrolyte membrane fuel-cell type systems.¹

Recent research works have indicated that 2-propanol had higher current densities and lower oxidation potential than methanol.^{2,3} 2-propanol fuel cells exhibit lower catalyst loadings and higher performance than DMFC (direct methanol fuel cells) at 90 and 60 °C operating temperatures at current densities lower than 200 mA/cm². In addition, higher open circuit voltages than methanol fuel cell were observed using Nafion®-117 and thick sulfonated polyetherketone membrane electrolytes.⁴⁻⁷

General behavior of cross over currents and open circuit potential in direct methanol and 2-propanol fuel cells

In order to see the general behavior of alcohol crossover and open circuit potential in direct methanol and 2-propanol fuel cells, literature values were collected and compared in Tables 1 and 2. At constant temperature, open circuit potential and crossover current increase with alcohol concentration in direct methanol fuel cell (Table 1). On the other hand, in direct 2-propanol fuel cells although cross-over current increases, open circuit potential drops slightly with alcohol concentration at constant temperature. At constant 2-propanol concentration, both cross-over current and open circuit potential increase with increasing operating temperature (Table 2). It is also seen that direct 2-propanol fuel cell has higher open circuit potentials and lower cross-over currents than direct methanol fuel cell.

Table 1. Collected literature values of various OCV and cross-over currents for methanol fuel cell.

| T(°C) | Methanol | | | | | |
|-------|-----------------------|-----------------------------------|---|-----------------------------------|----------------------|-----------------------------------|
| | 0.5 M | | 1 M | | 2 M | |
| | OCV(V) | J crossover (mA/cm ²) | OCV(V) | J crossover (mA/cm ²) | OCV(V) | J crossover (mA/cm ²) |
| 40 | - | - | 0.562 ^{b[6]} | - | - | - |
| 60 | 0.615 ^{b[6]} | 153.2 ^{[6]b} | 0.574 ^{b[6]} | 254.4 ^{b[6]} | - | - |
| 70 | 0.63 ^{a[8]} | - | 0.85 ^{a[8]} | - | 0.88 ^{a[8]} | - |
| 80 | 0.61 ^{a[8]} | - | 0.63 ^{a[8]} 0.583 ^{b[6]} | - | 0.85 ^{a[8]} | - |
| 90 | 0.57 ^{a[8]} | - | - | - | 0.75 ^{a[8]} | - |

Despite the advantages mentioned in Tables 1 and 2, the use of 2-propanol as a fuel for a direct alcohol fuel cell is limited due to the slow reaction rate and poisoning by intermediate species like acetone.⁹⁻¹¹

In this study, in order to see the advantages and limitations of direct 2-propanol fuel cell against direct methanol fuel cell, the effect of cell operating temperature, 2-propanol concentration, current load, and operating time on 2-propanol fuel cell performance were examined and compared with the general behavior of direct methanol fuel cell performance parameters collected from literature. 2-propanol fuel cell performance parameters

were extracted using an improved semi-empirical equation.¹² In addition, the effect of operating conditions (operating temperature and alcohol concentration) on the fuel cell model parameters were investigated.

Table 2. Collected literature values of various OCV and cross-over currents for 2-propanol fuel cell.

| | | 2-propanol | | | | |
|-------|-----------------------|--|-----------------------|--|-----------------------|--|
| T(°C) | 0.5 M | | 1 M | | 2 M | |
| | OCV(V) | $J_{crossover}$ (mA/cm ²) | OCV(V) | $J_{crossover}$ (mA/cm ²) | OCV(V) | $J_{crossover}$ (mA/cm ²) |
| 40 | - | - | 0.733 ^{b[6]} | 58.7 ^{b[6]} | - | - |
| 60 | 0.748 ^{b[6]} | 53.8 ^{b[6]} | 0.747 ^{b[6]} | 99.5 ^{b[6]} | 0.725 ^{b[6]} | 148.0 ^{b[6]} |
| 80 | - | - | 0.749 ^{b[6]} | 138.3 ^{b[6]} | - | - |

a. Anode: 35 wt%Pt -15 wt%Ru (2 mg.cm⁻² metal loading) dispersed on carbon (ketjen), Anode side solution flow rate: 1.12 cm³/min

b. The data were taken at an air flow rate of 643 ml/min. Crossover current was measured at 0.93 V. 2-propanol and methanol flow rate 38 ml/min, NM: not measured, Anode catalyst: Pt/Ru , 4.8 mg/cm²

The semi-empirical equation used in our study was developed by Argyropoulos et al., and Tu et al.^{12,13} The equation was developed from a simplified form for cell voltage for direct methanol fuel cell assuming that reduction of oxygen at the cathode does not proceed under mass transport limitations (Eq. (1)).

$$E_{cell} = E_O^* - b_{cell} \cdot \log j - R_e j + C_1 \ln(1 - C_2 j) \quad (1)$$

Parameters like E_0^* , b , R_e , C_1 and C_2 in Eq. (1) help to determine the cause of performance drop. In order to develop Eq. (1), Butler-Volmer kinetic equation was used for methanol oxidation and oxygen reduction at the anode and cathode. Steady state mass transport conditions were assumed for both methanol and oxygen. In Eq. (1), E_0^* is a potential term that is related with the equilibrium potential for the DMFC overall reaction , the exchange current densities, and transfer coefficients of anodic and cathodic reactions. b_{cell} is the summation of Tafel slopes for methanol oxidation and oxygen reduction reaction. R_e is the internal cell resistance. C_1 is a parameter related with the transfer coefficient and order of methanol oxidation reaction. C_2 is the methanol oxidation reaction limiting current (current when methanol depletes at the surface of the anode electrode).

Equations like Eq. (1) are not adequate for direct alcohol fuel cell since alcohol cross over effect on the cell voltage loss is not taken into account. Therefore, new semi-empirical models like in Eq. (2) were developed for the effect of cross-over current. As seen in Eq. (2), crossover effect of alcohol was employed by crossover current at the open circuit condition ($I_{cross,OCP}$).¹² At the open circuit potential, cross over current is maximum and it was treated to be linearly decreasing with increasing current density:

$$E_{cell} = (E_{cell,0} + E_{cross,c}) - b_c \ln \left[\left(1 - \frac{I_{cross,OCP}}{I \lim} \right) \cdot I + I_{cross,OCP} \right] \\ + E_{cross,a} - b_a \ln(I) + m_a \ln \left(1 - \frac{I}{I \lim} \right) - R_{cell} \cdot I \quad (2)$$

In Eq.(2), the term $E_{cell,0}$ denotes the difference between the half-cell potentials of the anode and cathode at the exchange current density i_o corrected by the thermodynamic effect of temperature. $E_{cross,a}$ and $E_{cross,c}$ denote intrinsic voltage loss due to alcohol crossover at the anode and cathode. $I_{cross,OC}$ is the apparent current density resulting from crossover at the open circuit potential. I_{lim} is the limiting current density and m_a is related to mass transfer and defined to be the reaction order multiplied by the Tafel slope. R_{cell} is the internal cell resistance. In Eq. (2) it was assumed that the mass transfer effect at the cathode side is minor compared to anode side, which dominates overall mass-transfer overpotential.

Parametric analysis for direct methanol fuel cell

A detailed parametric analysis for direct methanol fuel cells can be seen in Table 3. At 70 and 90 °C operating temperatures, crossover effect decreases as the alcohol concentration increases. In Table 3, squares in gray show the optimum collected parameters from the literature for different operating conditions. According to the collected optimum parameters for direct methanol fuel cells, open circuit potential was maximum at 90 °C and 0.125 M concentration. Crossover effect was minimum at 60 °C and 0.5 M concentration. Activation overpotential (b_{cell}) was minimum at 40 °C, 0.75 M and 70 °C, 0.125 M operating conditions. Table 3 shows that, generally it is more advantageous to operate direct methanol fuel cell at 70 °C.

In the model E_{MC}^o and α represent the methanol crossover effect and mass transport overpotential respectively. α has a major effect in the mass transport region.

Experimental

2-propanol fuel cell performance experiments were conducted in the set up shown in Figure 1. Operating temperature of fuel cell between 40-80 °C is controlled by an on-off temperature controller. Graphite blocks with serpentine flow channels were heated using a heating rod connected to the variac. The fuel cell was heated up to the desired operating temperature at open circuit with 2-propanol solution circulating through the anode compartment and dry air flowing through the cathode compartment.

By dissolving 2-propanol (Merck Chem.) in deionized water, 0.5 M, 1 M, and 2 M aqueous solutions of 2-propanol were prepared. Fuel at different 2-propanol concentrations (0.5 M, 1 M, and 2 M) was injected through the anode at a flow rate of 4 ml/min using a peristaltic pump with zero back pressure. Dry air was fed to the cathode at a flow rate of 25 ml/min with zero back pressure.

Membrane electrode assemblies with an active area of 5 cm² (Figure 1) were prepared as described elsewhere¹⁵ and mounted into the fuel cell hardware (Electrochem. Inc.). Catalyst loading on the electrodes were 1 mg/cm². For anode and cathode electrode, 20% Pt/C (Electrochem. Inc.) was used as an electrocatalyst. Nafion 117 was used as a proton conducting membrane.

For the polarization of fuel cell, 20 k Ω variable resistor was connected in series to an ammeter. By changing the resistance between anode and cathode, current was recorded by the ammeter and the voltage was recorded by a voltmeter, which was connected in parallel to the fuel cell assembly.

Table 3. Literature data for parameter estimation in direct methanol fuel-cell based on different models.

| Parameter | 40°C | | 60°C | 70°C | | | 90°C | | |
|--|---------------------------------|--------------------|---------------------------------|--|--|--|--|-----------------------------|--|
| | 0.5M | 0.75M | 0.5M | 0.25M | 0.5M | 0.125M | 0.25M | 0.5M | 0.125M |
| E_o^* (V) | 0.6798^b [14] | $\sim 0.225^a$ [8] | 0.6821^b [14] | 0.37^a [8] 0.6998^b [14] | 0.35^a [8] 0.6887^b [14] | 0.39^a [8] 0.6936^b [14] | 0.41^a [8] 0.7334^b [14] | 0.4^a [8] | 0.45^a [8] 0.7419^b [14] |
| E_{MC} (V) | 12.4608^b [14] | - | 9.8046^b [14] | 24.8149^b [14] | 16.481^b [14] | 52.0001^b [14] | 16.7081^b [14] | - | 26.4902^b [13] |
| R($\Omega \cdot \text{cm}^2$) | 3.6108^b [14] | 0.49^a [8] | 2.8169^b [14] | 0.1^a [8] 2.5476^b [14] | 0.1^a [8] 0.8810^b [14] | 0.1^a [8] 4.7548^b [14] | 0.05^a [8] 4.0383^b [14] | 0.05^a [8] | 0.05^a [8] 3.3587^b [14] |
| B_{cell} (V/dec) | 0.3621^b [14] | 0.109^a [8] | 0.2872^b [14] | 0.118^a [8] 0.7973^b [14] | 0.118^a [8] 0.6696^b [14] | 0.118^a [8] 0.1972^b [14] | 0.124^a [8] 0.3830^b [14] | 0.124^a [8] | 0.124^a [8] 0.2390^b [14] |
| I_{lim} (1/C2) (A/cm ²) | - | - | - | 0.05^a [8] | 0.1^a [8] | - | 0.1^a [8] | 0.2^a [8] | - |
| m_a (C1) (V) | - | 0.05^a [8] | - | 0.059^a [8] | 0.07^a [8] | 0.085^a [8] | 0.07^a [8] | 0.12^a [8] | 0.12^a [8] |
| $\kappa_{b(A/cm^2)^{-1}}$ | 7.2109^b [14] | - | 5.5202^b [14] | 18.5831^b [14] | 4.1893^b [14] | 50.7664^b [14] | 10.2502^b [14] | - | 22.9693^b [14] |
| $\alpha \times 10^3$ (K.cm ² /A) | -4.0232^b [14] | - | -0.8185^b [14] | -7.8302^b [14] | -0.4176^b [14] | -3.8307^b [14] | -2.0918^b [14] | - | -2.1155^b [14] |

^a Anode35wt%Pt 15wt%Ru on C, cathodePt black, solution flowrate 1.12cm³/min, air feed cathodes pressurized at 2atm

$$\text{Model: } E_{cell} = E_o^* - b_{cell} \cdot \log j - R_e \cdot j + C_1 \cdot \ln(1 - C_2 \cdot j)$$

$$E_o^* = E_{O_{cell}} - \frac{RT}{\alpha_c F} \ln \left(\frac{p_O^{ref}}{j_{O_c} \cdot (pO)^{NO}} \right) - \frac{RT}{\alpha_a F} \ln \left(\frac{C_{ME}^{ref}}{j_{O_c} \cdot C_{ME}^N} \right), \quad b_{cell} = \frac{2.303RT}{F} \left(\frac{1}{\alpha_a} + \frac{1}{\alpha_c} \right)$$

$$C_1 = \frac{NRT}{\alpha_a F}, \quad C_2 = \frac{1}{I_{lim}} = \frac{1}{nFk_{eff} \cdot C_{ME}}$$

j is the current density, α_a and α_c the transfer coefficients for the oxidation of methanol and reduction of oxygen, respectively, R_e the internal cell resistance (mainly due to the polymer electrolyte membrane), N a reaction order for methanol oxidation, k_{eff} an effective mass transport coefficient for the anode side of the cell, C_{ME} the methanol concentration and pO is the oxygen pressure. E_o^* cell is the standard potential for the DMFC overall reaction, which theoretically is given by the Nernst equation.

^b Anode35wt%Pt 15wt%Ru on C, cathodePt black, solution flowrate 1.12cm³/min, air feed cathodes pressurized at 2atm

$$\text{Model: } E_{cell} = E_o - b \cdot \ln[1 - \kappa_b \cdot j] - R_{cell} \cdot j - E_{MC}^o \cdot \left(1 - \exp \left(\frac{-\alpha \cdot j}{T} \right) \right)$$

In the model E_{MC}^o and α represent the methanol crossover effect and mass transport overpotential respectively. α has a major effect in the mass transport region.

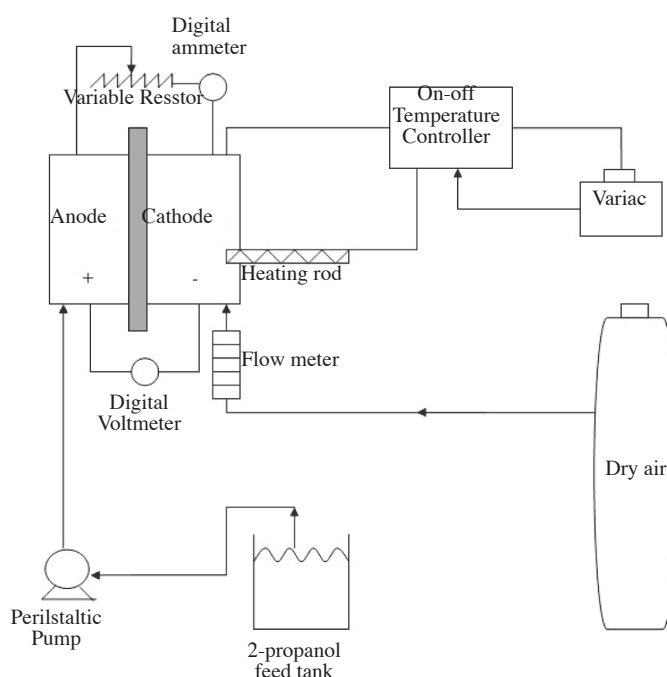


Figure 1. 2-Propanol fuel cell test system.

Results and discussion

Power curves and practical efficiency

Power curves of 2-propanol fuel cell at different operating temperatures are depicted in Figure 2. Highest power density was achieved at 80 °C and 1 M alcohol concentration. Although the maximum power density increased with increasing alcohol concentration at 40 °C, an opposite behavior was observed at 60 and 80 °C. If the fuel cell is operated at the maximum power density, the highest practical efficiencies would be at 60 °C and 2 M and at 40 °C and 1 M (Figure 3). Practical efficiency at the maximum power density can be defined as in Eq. (3).

$$\eta_{\text{practical}} = E_{\text{appliedatmaximumpower}} / E_{\text{OCV}} \quad (3)$$

In Figure 3, it is seen that practical efficiency shows a different behavior than power density. At 40 °C, practical efficiency shows maxima. At 60 °C practical efficiency increases and at 80 °C practical efficiency decreases with increasing 2-propanol concentration. The relation between practical efficiency, power density, and 2-propanol concentration can be understood better after the parameter estimation given in the next section.

Parameter estimation

At 80 °C it was seen that practical efficiency was lowest at 2 M alcohol concentration. In addition, power densities at 2 M concentration were lower than 1 M concentration. This means that although voltage drop is highest at 2 M feed concentration, higher current densities than 0.5 M concentration were achieved. This behavior

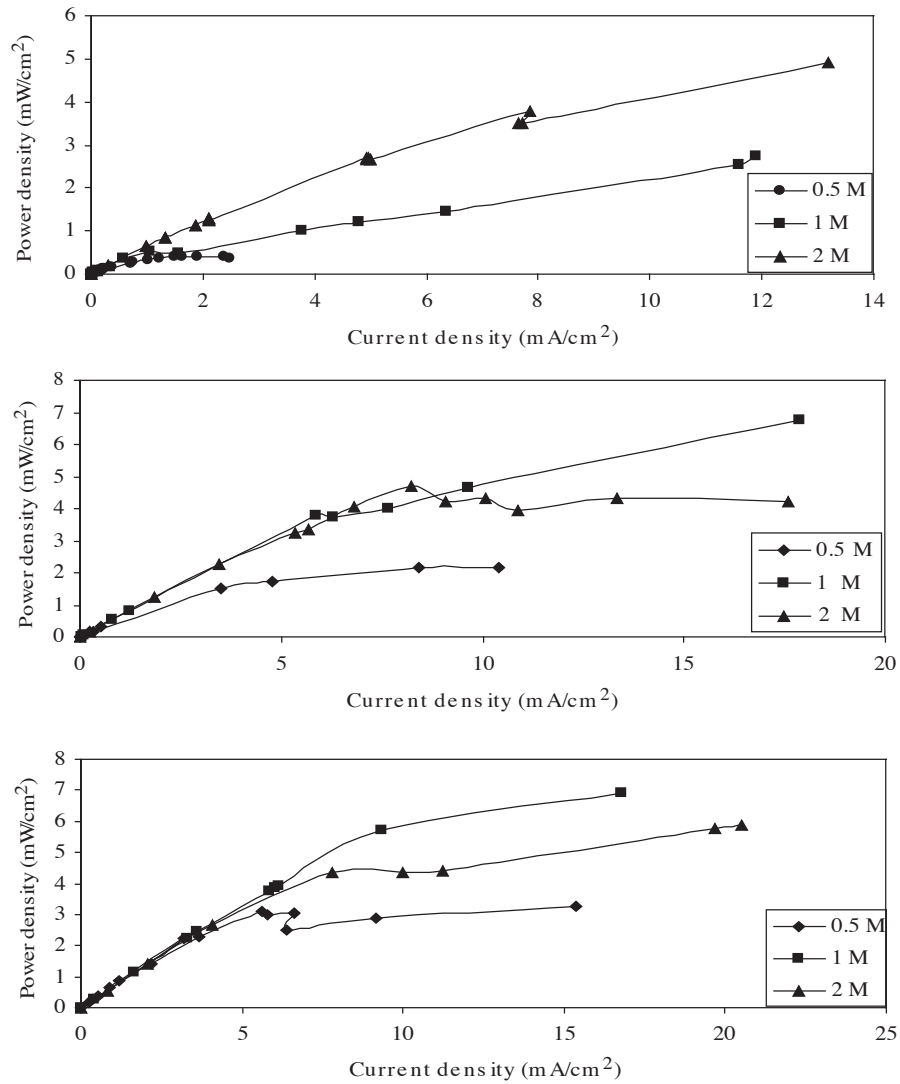


Figure 2. Cell power density change with current density. $T = 80\text{ }^{\circ}\text{C}$ Dry air flowrate: 25 ml/min, alcohol flow rate: 4 ml/min. (a) 40 °C, (b) 60 °C, (c) 80 °C.

at 2 M concentration can be explained better after parameter estimation from the polarization curves. Effect of operating conditions on kinetic parameters like Tafel slope (for alcohol oxidation and oxygen reduction) can be extracted after fitting model Eq. (2) on polarization curves. Polarization curves were repeated twice at every operating condition and they were reproducible. For the parameter estimation non-linear least square method using the Levenberg Marquardt algorithm in Polymath software was used. For all the operating conditions, parameters were estimated at a 95% confidence interval, and the correlation coefficients were at least 0.9.

If extracted parameters in Table 4 are analyzed, it can be seen that, the anodic Tafel slope (b_a), and mass transfer overpotential (m_a) are the lowest for 1 M and highest for 0.5 M at 80 °C. This means that alcohol oxidation and mass transfer rates are fast at 1 M, which causes high current and power densities. On the other hand, alcohol oxidation and mass transfer rates are slow at 0.5 M causing low current and power densities.

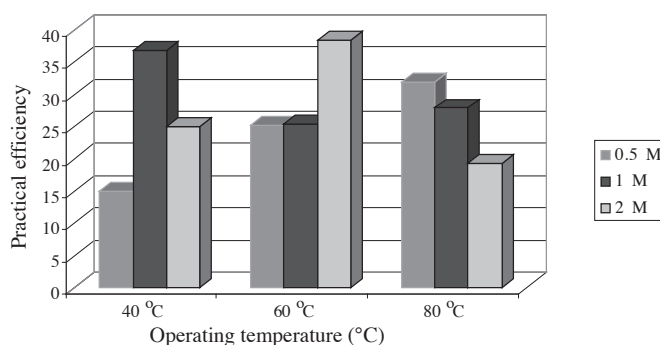


Figure 3. Practical efficiency at maximum power density .Dry air flow rate: 25 ml/min, alcohol flow rate: 4 ml/min.

Table 4. Parameter estimation for 2-propanol fuel cell based on Eq. (2).

| Parameter | 40 °C | | | 80 °C | | | | | |
|--|-----------------------|-----------------------|-----------------------|------------------------|---------|--------|-----------------------|---------|--------|
| | 0.5 M | 1 M | 2 M | 0.5 M | 1 M | 2 M | 0.5 M | 1 M | 2 M |
| A(V) ^a | 0.404 | 0.577 | 0.528 | 0.516 | 0.563 | 0.551 | 0.549 | 0.579 | 0.528 |
| R(Ohm) | 3.01 | 4.53 | 4.53 | 3.33 | 4.03 | 4.53 | 4.53 | 5.03 | 5.04 |
| ba (V/dec) | 0.014 | 0.017 | 0.023 | 0.020 | 0.024 | 0.0269 | 0.029 | 0.0096 | 0.021 |
| bc (V/dec) | 0.0095 | 0.0097 | 0.017 | 0.006 | 0.018 | 0.024 | 0.022 | 0.047 | 0.029 |
| J _{crossover} (A/cm ²) | 4.06×10 ⁻⁶ | 2.55×10 ⁻⁴ | 4.99×10 ⁻⁴ | 1.183×10 ⁻⁵ | 0.0026 | 0.0038 | 4.52×10 ⁻⁴ | 0.0075 | 0.0017 |
| I _{lim} (A/cm ²) | 0.00276 | 0.0164 | 0.0227 | 0.0124 | 0.02648 | 0.0224 | 0.01295 | 0.01697 | 0.0307 |
| ma(V/dec) | 0.374 | 0.667 | 0.523 | 0.44 | 0.404 | 0.538 | 0.646 | 0.0963 | 0.512 |

^a $A = E_{cello} + E_{cross,c} + E_{cross,a}$ as given in Eq. (2)

Therefore, it seems that direct 2-propanol fuel cell performance that was shown in Figure 2 has close relation with alcohol oxidation electrokinetics and mass transfer rate. Same kind of relation can be formed at other operating temperatures like 80 °C.

At 40 °C, the highest practical efficiency (Figure 3) at 1 M and the highest power density at 2 M (Figure 2) can be explained with the highest value of open circuit potential term (A(V)) and the highest value of limiting current density in Table 4. At 60 °C, the highest power density at 1 M (Figure 2) can be explained with the highest value of open circuit potential term (A(V)) and the highest value of limiting current density in Table 4.

Optimum parameters (painted in gray) in Table 4 show that open circuit is maximum, anodic activation and mass transfer overpotential are minimum at 80 °C, 1 M operating conditions. Crossover current is minimum at 40 °C, 0.5 M operating conditions. If the optimum conditions for methanol (Table 3) and 2-propanol fuel cell are compared, it can be seen that crossover is minimized at lower temperatures in 2-propanol fuel cell.

In Figure 4, behavior of cross-over current at open circuit potential (after parameter estimation shown

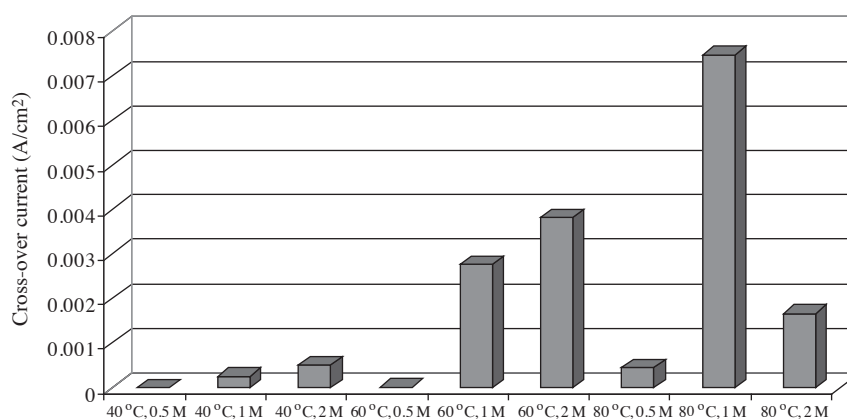
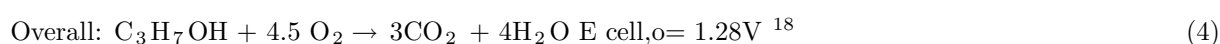
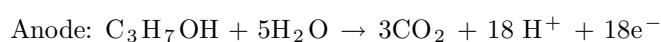


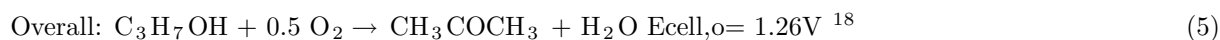
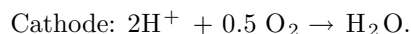
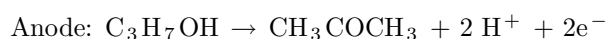
Figure 4. Cross-over current for 2-propanol fuel cell at different conditions.

in Table 4) can be seen at different operating conditions. As the alcohol concentration increases at constant operating temperature, cross-over current increases. However, at 80 °C, this behavior was not observed. This may be due to cross-over currents that are directly related with the swelling properties of the Nafion membrane in direct alcohol fuel cell. Swelling of membrane or solvent uptake depends on the alcohol concentration. At room temperature, it was seen that solvent uptake of Nafion 117 gives is maxima at a certain 2-propanol mole fraction.¹⁶ Therefore, lower cross-over currents estimated at 2 M and 80 °C could be due to decreasing of solvent uptake with increasing alcohol concentration after a maxima. Since alcohol crossover could be limited at 2 M concentration, lower cross over currents may have been obtained.

Open circuit potential

In order to understand the behavior of the open circuit potential in 2-propanol fuel cell, initially the theoretical dependence of reversible cell potential on temperature was determined based on two different overall cell reactions (Eqs. (4) and (5)).⁹ First reaction is complete oxidation of 2-propanol to carbon dioxide (Eq. (4)) and the second reaction is the electrochemical dehydrogenation of 2-propanol to acetone (Eq. (5)). In the literature, these two reactions are generally considered to be in parallel with 2-propanol fuel cell.^{6,7} In order to determine the theoretical dependence of reversible cell potential on temperature (Eq. (6)), standard entropy change of two overall reactions (Eqs. (4) and (5)) were calculated from the formation entropies of each individual reactant and product.^{17,18} In order to see the effect of phase change, theoretical dependence of reversible cell potential on temperature were calculated for different phases of 2-propanol and water (Figure 5). Figure 5 shows that if the cross-over effect is neglected, the reversible cell potential increases with temperature. For instance, for a fuel cell fed with liquid 2-propanol and forming liquid phase water product, every 10 K rise in fuel cell temperature corresponds approximately to 10 mV rise in reversible cell potential.





$$\left(\frac{\partial E^o}{\partial T}\right)_P = \frac{\Delta S_{rxn}^o}{nF}$$
 (6)

In order to see the effect of temperature and 2-propanol concentration on the open circuit voltage, fuel cell was kept at least 5 min at zero current density to stabilize open circuit potential. Open circuit data acquisition was repeated several times and all open circuit data at different operating temperatures and alcohol concentrations were reproducible as presented in Figure 6.

The effect of cell temperature on open circuit potential at different concentrations shows discrepancies. It is clearly seen in Figure 5 that theoretically the reversible cell voltage increases with increasing operating temperature at approximately 1 mV/K. In Figure 6, this theoretical dependence of open circuit potential was not seen at 0.5 M. or 2 M alcohol concentrations. This means that there may be other factors that affect the temperature dependence of open circuit potential. One of these factors could be the cross-over effect.

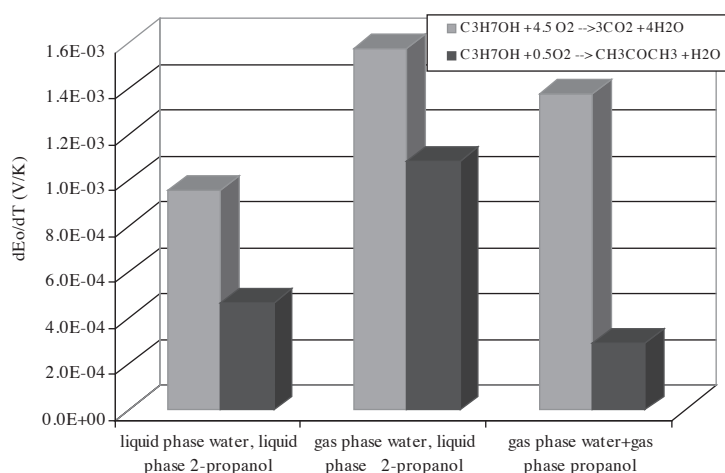


Figure 5. Reversible cell potential dependence on temperature at different phases of reactants and products.¹⁸.

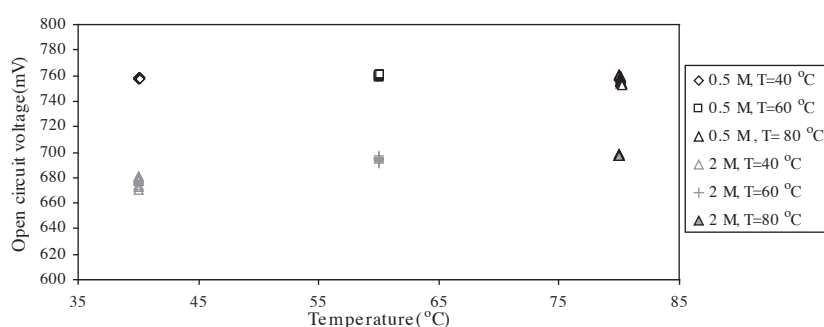


Figure 6. Effect of operating temperature on the open circuit voltage at various alcohol concentrations. Dry air flow rate: 25 ml/min, alcohol flow rate: 4 ml/min.

Voltage drop under current load

Generally, in 2-propanol fuel cells, high cell voltage drop is observed in 300 s at high current densities due to faster poisoning of the anode surface.⁵ In other words, the effect of poisoning was observed at shorter operating times at high current loads.⁶ Anode poisoning may be caused due to electrochemical oxidation or dehydrogenation of 2-propanol to acetone. At current densities less than 100 mA/cm², dehydrogenation reaction dominates. After dehydrogenation, evolved H₂ gas is depleted by electrooxidation. At low potentials, electrochemical oxidation of 2-propanol to acetone dominates. Therefore, build up of acetone in the membrane/anode interface leads to voltage loss and cause mass transport resistance.^{6,7}

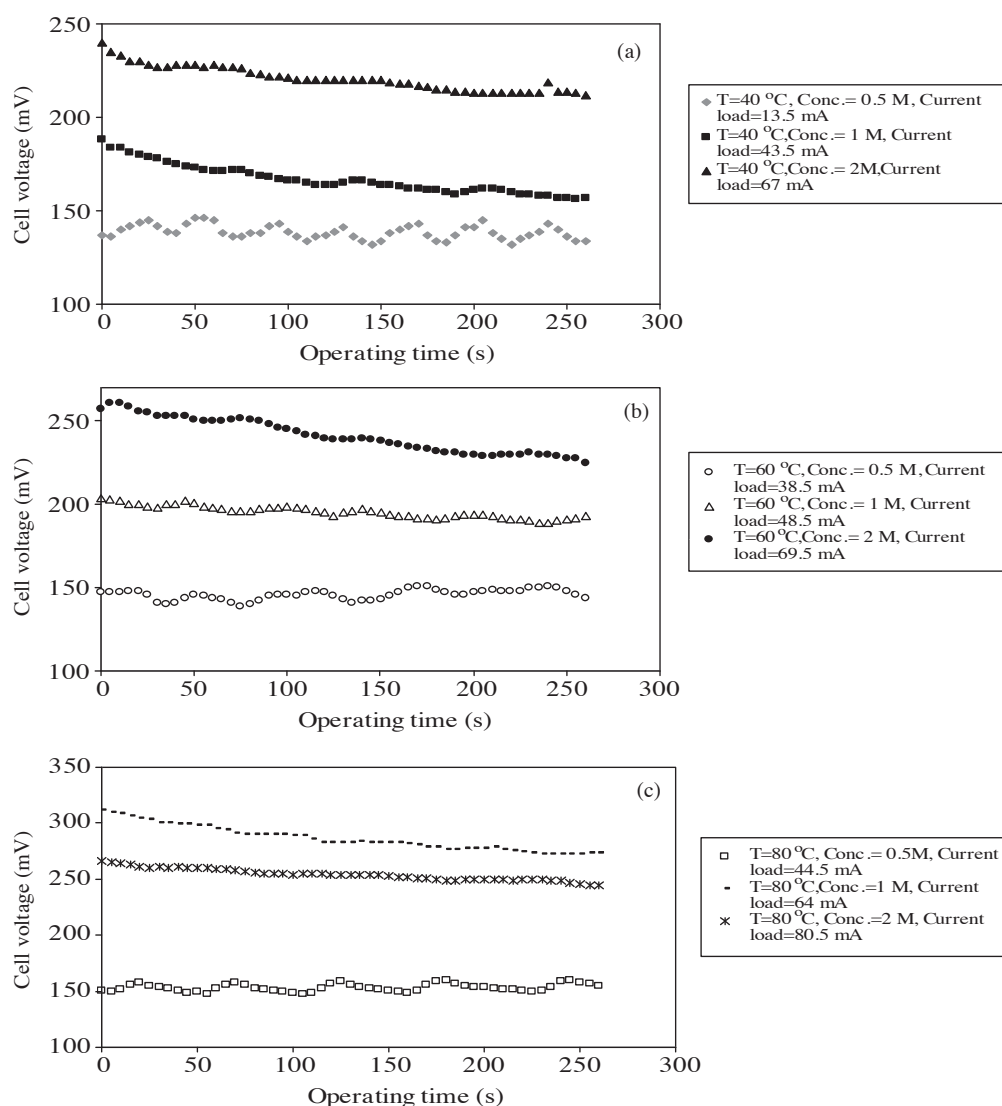


Figure 7. Cell operating voltage change with operating time at the maximum attainable current load conditions. Dry air flow rate: 25 ml/min, alcohol flow rate: 4 ml/min. (a) T = 40 °C, (b) T = 60 °C, (c) T = 80 °C.

Figure 7 shows the fuel cell stability with time at the maximum current load conditions at different temperatures and alcohol concentrations. Although no drastic performance loss of the fuel cell was observed, if the voltage drops in 250 s were analyzed, it was clearly seen in Figure 8 that the most stable fuel cell performance was achieved at 0.5 M alcohol concentration. Figure 8 also shows that fuel cell may not be operated effectively at 60 °C, 2 M and 80 °C, 1 M conditions since poisoning of the anode is faster.

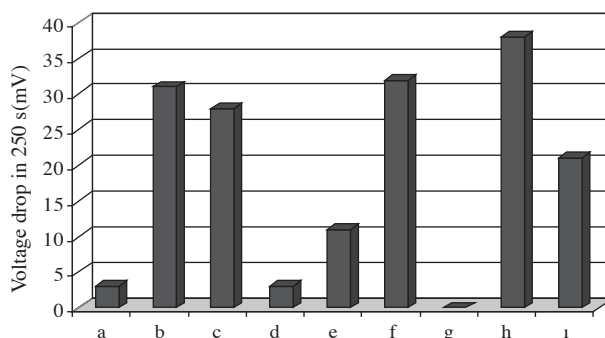


Figure 8. Voltage drop in 250 sec for different cell conditions , (a: T = 40 °C, Conc.= 0.5 M, Current load = 13.5 mA, b: T = 40 °C, Conc. = 1 M, Current load = 43.5 mA, c: T= 40 °C, Conc. = 2 M, Current load = 67 mA, d: T = 60 °C, Conc.= 0.5 M, Current load = 38.5 mA, e: T = 60 °C, Conc. = 1 M, Current load = 48.5 mA, f: T = 60 °C, Conc. = 2M, Current load = 69.5 mA, g: T = 80 °C, Conc. = 0.5 M, Current load = 44.5 mA, h: T = 80 °C, Conc. = 1 M, Current load = 64mA, i: T = 80 °C, Conc. = 2 M, Current load = 80.5 mA.).

Conclusions

According to the performance analysis, 2-propanol fuel cell shows the highest performance at 1 M concentration and 80 °C operating temperature. Highest practical efficiency at the maximum power density is achieved at 2 M and 60 °C and cross-over current is minimum at 0.5 M, 40 °C operating temperature. High performance at 1 M and 80 °C could be related with the low activation and mass transfer overpotentials. Membrane swelling properties could be effective in lower crossover currents estimated at 2 M and 80 °C operating conditions. 2-propanol fuel cell may not be operated effectively at 60 °C, 2 M and 80 °C, 1 M conditions due to high voltage drops at short operating times.

Nomenclature

| | |
|-------------|--|
| b | Tafel slope, mV/dec |
| E_o | Difference between half cell potentials, V |
| E_{cross} | Voltage loss due to alcohol cross over, V |
| F | Faraday constant, 96500 C/mol |
| I_{lim} | Limiting current, A |
| I | Current, A |

| | |
|--------------------|--|
| I_{cross} | Cross-over current, A |
| $J_{crossover}$ | Cross-over current density, mA/cm ² |
| n | Number of equivalence |
| OCV | Open circuit potential, V |
| P | Pressure |
| R | Cell resistance, ohm |
| ΔS_{rxn} | Entropy change of reaction, J/mol.K |
| T | Temperature , K |
| $\eta_{practical}$ | Practical efficiency |
| n | Number of equivalence |

References

- Demirci, U. B. *J. Power Sources*. **2007**, *169*, 239–246.
- Gonzales, M.J.; Hable , C.T.; Wrighton, M.S., *J. Phys. Chem. B* **1998**, *102*, 9881-9890.
- Qi, Z.; Hollet, M., Attia, A.; Kaufman, A., *Electrochemical Solid-State Lett.* **2002**, *5* , A129-A130.
- Fujiwara, N.; Siroma, Z.; Ioroi, T.; Yasuda, K. *J. Power Sources* **2007**, *164*, 457–463.
- Qi, Z. ; Kaufman, A. *J. Power Sources* **2002**, *112*, 121-129.
- 6 Qi, Z. ; Kaufman, A. *J. Power Sources* **2003**, *118*, 54-60.
- Cao D.; Bergens, S. H. *J. Power Sources* **2003**, *124*, 12–17.
- Scott, K.; Jackson, C.; Argropoulos , P. *J. Power Sources* **2006**, *161*, 885-892.
- Otomo, J.; Li, X.; Kobayashi, T.; Wen, C.; Nagamoto, H.; Takahashi, H. *J. Electroanal. Chem.* **2004**, *573*, 99–109.
- Sun, S.-G.; Lin, Y. *Electrochim. Acta* **1996**, *41*, 693-700.
- Sun, S.-G.; Lin, Y. *Electrochim. Acta* **1998**, *44*, 1153-1162.
- Tu, H-C.; Wang ,Y-Y.; Wan, C-C.; Hsueh, K-L. *J. Power Sources* **2006**, *159*, 1105–1114.
- Argyropoulos, P.; Scott., K.; Shukla, A.K.; Jackson, C. *J. Power Sources* **2003**, *123*, 190–199.
- Kim, T.H.; Bae, Y.C. *Polymer* **2005**, *46*, 6494-6499.
- Tapan, N.A.; Kök, A. *Chem. Eng. Commun.* **2009**, *196*, 131-147
- Saarinen, V.; Kreuer, K.D; Schuster, M.; Merkle, R.; Maier, *Solid State Inics* **2007**, *178*, 533-537.
- Fuel cell Handbook*, EG&G Services; Parsons, Inc; Science Applications International Corporation; developed for the National Energy Technology Laboratory, Office of Fossil Energy, U.S. Department of Energy , Morgantown, West Virginia, 2000.
- Burgess, D.R., “Thermochemical Data” in *NIST Chemistry WebBook, NIST Standard Reference Database Number 69*; Linstrom, P.J.; Mallard, W.G, Eds.; National Institute of Standards and Technology, Gaithersburg MD, 2008.